

MICRO-SCALE ELECTRON BEAM GENERATION USING PYROELECTRIC CRYSTALS

R. B. Yoder*, Z. Kabilova

Goucher College, Center for Natural Sciences, Baltimore, Maryland 21204, USA

Abstract

Novel laser-powered acceleration structures currently under development, which have dimensions comparable to optical wavelengths and can be constructed on a silicon wafer, require injection of a sub-micron-scale electron bunch to achieve high-quality, monoenergetic output beams. A potential injection mechanism for such micro-scale beams relies on field emission from a nanotip array, followed by acceleration to near-relativistic energies. We demonstrate field emission of electrons from a lithium niobate crystal during heating and cooling, and describe the production of electrons within a hollow channel along the axis of a lithium niobate crystal. Measurements of emitted beam properties are compared with direct measurements of crystal fields under comparable conditions and modeled mathematically.

INTRODUCTION

Microscale high-gradient acceleration structures currently in development, such as dielectric laser accelerators (DLAs) [1–3], represent a possible path to optical acceleration of electrons on a chip, potentially allowing enormous reduction in the footprint and cost of both industrial linacs and colliders. Such accelerators have structure dimensions on the order of the drive laser wavelength, requiring beam injection and diagnostics to be carried out on the same scale. Though proof-of-concept experiments to date [2, 3] have used conventional beams which overfill the structures, efficient and monoenergetic acceleration in a DLA will require the injection or production of sub-micron-scale electron bunches—well beyond the capabilities of conventional rf photocathode guns.

A second challenge for optical acceleration structures is that their efficiency and effectiveness tend to be maximal for fully relativistic particles, that is, when $v \sim c$. While DLAs can be adapted for subrelativistic operation [4, 5], the requirement of phase synchronism for acceleration then demands that the effective phase velocity in the structure be less than c . This requirement necessarily introduces transverse fields that would otherwise be suppressed, leading to defocusing as well as greatly reduced gradient. Injection at near-relativistic energies (near several hundred keV, or $\beta = v/c \sim 0.8$) greatly reduces the difficulty of transporting beam into and through the structure.

We report in this paper on progress toward development of an injector concept that addresses both of these challenges: local field production using pyroelectric crystals (or arrays) combined with field emission from microscale sources. In this concept, we obtain strong quasi-DC fields in a dielectric

environment—without applying external voltage—via heating and cooling pyroelectric crystals, which then cause both emission and pre-acceleration of electrons to near-relativistic energies. Pyroelectrics (e.g. crystalline ferroelectrics such as LiNbO_3 , LiTaO_3 , and BaTiO_3) are a class of materials that develop spontaneous charge polarization while in a nonequilibrium thermal state, producing surface charges on their $\pm Z$ faces during heating and cooling. Large charges (tens of nC per cm^2) can be obtained with relatively small temperature changes, and relaxation to the equilibrium state is extremely slow ($\tau \sim 10^5$ – 10^7 sec) [6]. Accordingly, pyroelectric crystals have been investigated as acceleration methods, especially for radiation production (neutrons and x-rays) [7–9]. Crystal polarization is fully reversible and repeatable indefinitely, implying that periodic operation at a slow repetition rate can be achieved by regular thermal cycling.

As dielectric materials, pyroelectrics can themselves be used as substrates for emitter deposition, and can also be themselves patterned with nanoscale emitting features via, for example, focused-ion-beam (FIB) milling. Field emission from nanotips constructed on a LiNbO_3 crystal have been investigated [10], and in general nanotip arrays can be patterned or deposited on a semiconducting substrate, making them compatible in both scale and materials with DLA approaches. Carbon nanotubes (CNTs) have also been effectively used for high-current photocathodes [11], and can also be patterned or grown on wafers.

EMISSION MEASUREMENTS

Crystal Thermal Behavior and Field Production

In previous work [12], the time-dependent temperature behavior and field production were measured and modeled for 1 cm^3 lithium niobate crystals. Charge production on the surface of a pyroelectric crystal is determined by its temperature change: surface charge density $\sigma = \pm P_s = \gamma \Delta T$, where P_s is the material polarization, ΔT is the temperature change, and γ is known as the pyroelectric coefficient for a given material ($\gamma \approx 10 \text{ nC/cm}^2/\text{K}$ for LiNbO_3 .) Once produced, the surface charge then dissipates over time via bulk conduction, surface transport, or (potentially) ionization or flashover in the surrounding medium. The total surface charge then varies with time according to

$$\frac{dQ}{dt} = \gamma A \frac{dT}{dt} - \frac{1}{R_{\text{eff}} C} Q \quad (1)$$

where A is the area of a face, and R_{eff} , C are the effective resistance and capacitance between the crystal faces, respectively.

* rodney.yoder@goucher.edu

The very poor thermal conductivity of pyroelectric materials must be taken into account when heating [12, 13]. Since the surface charge tracks the changing temperature at the surface, which is not the location of the heat source, the field produced will have a time structure dominated by the effects of the slow thermal diffusion. For larger crystals, the temperature variation on the upper (unheated) face can be fitted to a solution of the 1-dimensional heat equation, $dT/dt = \kappa(d^2T/dx^2)$, allowing an empirical measurement of the effective diffusivity κ of the bulk crystal. The 1D treatment becomes less rigorous for thinner crystal geometries at longer time scales (see Fig. 1).

The pyroelectric constant of our lithium niobate crystals in air has been measured at 13–15 nC/cm²/K, with effective relaxation times for charge and field production that are on the order of 1000–1200 s [12]. While the bulk resistivity of LiNbO₃ has been estimated at 10¹⁴–10¹⁶ Ω m [6], which would imply relaxation times of hours, our results imply that surface transport is a significant contribution to the discharge.

Field production was also measured directly by recording the deflection of a 20-keV electron beam in a modified scanning electron microscope (SEM) as it passed through an 8-mm gap between two 12 mm × 12 mm × 10 mm LiNbO₃ crystals, oriented with their ±Z faces opposite each other. Analytic estimates of the field strength for a given amount of deflection were verified through PIC simulation of the detailed geometry of the experiment using OOPIC. These field strengths can be further used to infer the net charge produced on each crystal face, as shown in Fig. 2.

The charges calculated in this way are roughly one order of magnitude lower than that predicted by literature values of the pyroelectric constant; however, we note that these *net* charges include both the surface pyroelectric charge and the effect of screening by charges and currents arising within the crystal bulk [6].

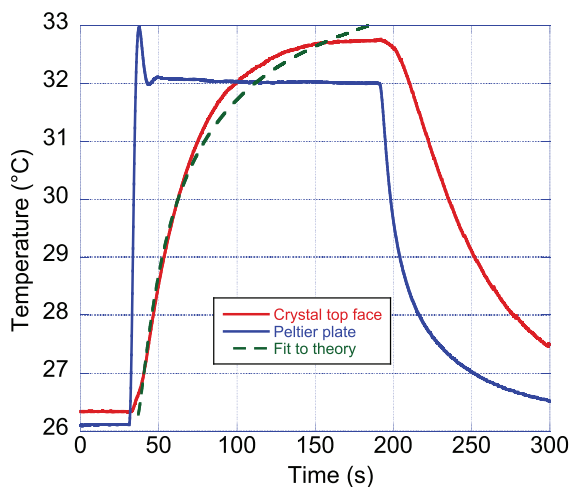


Figure 1: Temperature measurement, using thermistors, for our cylindrical LiNbO₃ crystal in vacuum, heated from below using a Peltier plate. The dashed curve is a fit to the heat equation, with $\kappa = 2.5 \pm 0.05$ mm²/s.

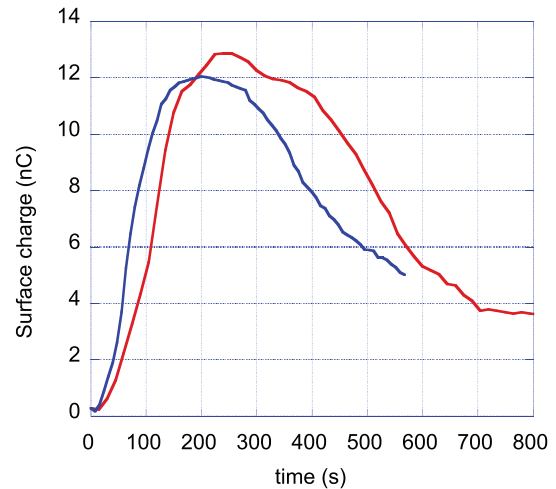


Figure 2: Surface charge (inferred from measured field strength) induced on 12 × 12 mm² LiNbO₃ crystals when heated by 5 °C, with heater temperature ramped linearly over 60 sec (blue) and 120 sec (red).

Based on these results, we find that the surface fields just at the crystal face, per degree temperature increase, are on the order of 2 kV/mm/K.

Single-Crystal Emission

As a first step toward demonstrating emission in an array, we have collected preliminary data on field emission from a single crystal in vacuum. A cylindrical LiNbO₃ crystal (Z-cut, 9 mm diameter × 1 cm height) is silver-plated on its +Z face and then coated in the center of that face with a layer of multi-wall carbon nanotubes (MWCNTs), forming an emitting region several mm wide. The MWCNTs, with lengths 2–4 μm and diameters 15–20 nm, are intended to provide a field enhancement factor β of several hundred, though they are randomly aligned, which may slightly depress the emitted current value.

The crystal is heated or cooled from its opposite (−Z) face using a Peltier plate, and emitted current is collected by a Faraday cup positioned a few mm from the CNT surface. A grounded shield isolates the cup, a phosphor coating surrounding the collector permits visual confirmation of current, and a retarding potential can be applied within the cup assembly for low-energy (< 5 keV) diagnostics. For these preliminary tests, the crystal was taken through heating and cooling cycles of 6–8 °C. Vacuum pressure during test runs was in the range of 10^{−8} torr.

Emitted current is expected to follow Fowler-Nordheim theory, with current density $J = aE^2 \exp(-b/E)$, where a and b are constants that depend on the material work function, and $E = \beta E_p$ is the effective field at the crystal surface, depending on the pyroelectric field E_p and the enhancement factor β . We therefore expect to see time-varying emission that tracks the changing surface charge on the crystal, but note that it will depend sensitively on the density and dimension of the CNTs via the value of β .

Typical emission results are presented in Fig. 3, showing emitted currents of a fraction of a nanoampere during heating cycles of $\pm 8^\circ\text{C}$. Note that the current “turns on” suddenly, after a threshold field is reached, but then slowly returns to zero as the surface charge dissipates. Given that field emission in photocathodes normally requires $\beta E_a = 2\text{--}10\text{ MV/mm}$ [14], and that our estimated surface fields without CNTs are $\sim 15\text{ kV/mm}$, we are relying on a CNT field enhancement factor of at least several hundred for emission.

Measurement of energy gain by emitted electrons is still in progress. A preliminary modeling study suggests that acceleration across a few mm to the Faraday cup is expected to produce 3 to 4 kV energy gain in emitted electrons, depending on separation distance, for 5°C temperature change. Applying a 1.5-kV retarding potential to the Faraday cup via an internal grid may have reduced the current for a portion of the pulse (Fig. 4).

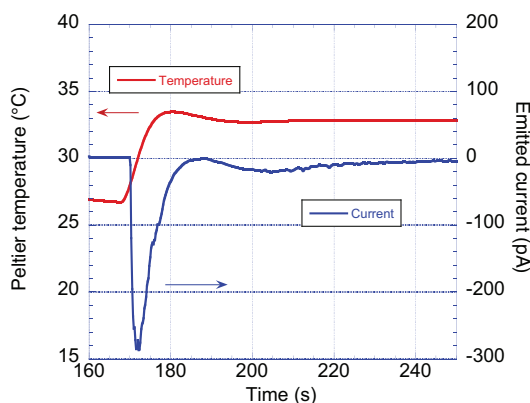


Figure 3: Sample emission signal from CNT-enhanced LiNbO_3 crystal when heated by 8°C . Emission is immediately suppressed when the fields change signs upon cooling.

EMISSION AND ACCELERATION IN A HOLLOW CHANNEL

To increase the output energy of emitted electrons, we have previously described a method for extending the acceleration region through staging of multiple crystals. We propose to employ a narrow acceleration channel that is drilled through the center of the crystal stack, connecting the $\pm Z$ faces, as shown in Fig. 5. The field strengths of a few kV/mm demonstrated above are sufficient to reach energies of $\sim 300\text{ keV}$ in a three-crystal stack. Our results above show that a CNT-based emitter is feasible for this concept.

FUTURE WORK

We have seen that pyroelectric crystal arrays can provide surface electrostatic fields on the order of several kV/mm per degree of temperature change. Once established, the fields

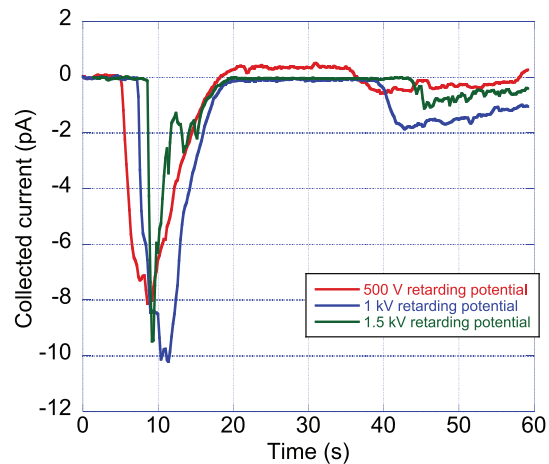


Figure 4: Emitted current on repeated thermal cycling by 6°C , with increasing retarding potential applied to the Faraday cup.

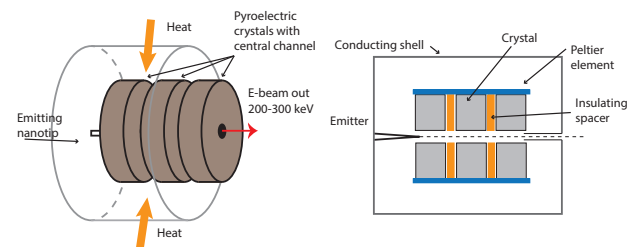


Figure 5: Concept drawing of pyroelectric stack accelerator, in different versions: cylindrically symmetric (left) and square or planar (right, in cross-section).

can remain nearly constant for hundreds of seconds before the crystal relaxes, and tailoring of the temperature profile can produce relatively constant fields. On the other hand, a train of pulses with slow repetition rate can be produced using an oscillating temperature profile. Such a method for producing high fields without a bulky external high-voltage supply is well suited to injectors for microaccelerators in general, but especially for stand-alone applications in which charge acceleration and radiation occur within a single device. Photoexcitation has also been shown to be possible for pulse or bunch train tailoring of pyroelectrics [15].

We plan to extend these preliminary emission measurements in the near future by including energy diagnostics and more fully characterizing the field profile of the single crystal. We intend eventually to demonstrate beam acceleration in a multi-crystal array.

ACKNOWLEDGMENT

Support for this work was provided by the Office of the Provost, Goucher College, and the Goucher Summer Science Research Program. J. Stevenson, P. Meyer, C. Gooditis, J. Sturgis, and B. Saeks contributed to earlier stages of this work.

REFERENCES

- [1] R. J. England *et al.*, “Dielectric laser accelerators,” *Rev. Mod. Phys.*, vol. 86, p. 1337, 2014.

- [2] E. A. Peralta *et al.*, “Demonstration of electron acceleration in a laser-driven dielectric microstructure,” *Nature*, vol. 503, p. 91, 2013.
- [3] R. B. Yoder *et al.*, “First acceleration in a resonant optical-scale laser-powered structure,” in *Proc. IPAC’15*, Richmond, VA, USA, May 2015, paper WEPWA053, p. 2624.
- [4] J. McNeur *et al.*, “A tapered dielectric structure for laser acceleration at low energy,” in *Proc. IPAC’10*, Kyoto, Japan, May 2010, paper THPD047, pp. 4387–4389.
- [5] J. Breuer and P. Hommelhoff, “Laser-based acceleration of nonrelativistic electrons at a dielectric structure,” *Phys. Rev. Lett.*, vol. 111, p. 134803, 2013.
- [6] G. Rosenman *et al.*, “Electron emission from ferroelectrics,” *J. Appl. Phys.*, vol. 88, p. 6109, 2000.
- [7] J. A. Geuther, Y. Danon, and F. Saglime, “Nuclear reactions induced by a pyroelectric accelerator,” *Phys. Rev. Lett.*, vol. 95, p. 054803, 2006.
- [8] M. Klopfer, V. Satchouk, A. Cao, T. Wolowiec, Y. Alivov, and S. Molloy, “Demonstration of a non-contact x-ray source using an inductively heated pyroelectric accelerator,” *Nucl. Instr. Meth. Phys. Res. A*, vol. 779, pp. 124–131, 2015.
- [9] J. D. Brownridge and S. Shafroth, *Appl. Phys. Lett.*, vol. 85, p. 1298, 2004.
- [10] E. R. Arab *et al.*, “Initial results on electron beam generation using pyroelectric crystals,” in *Proc. IPAC’10*, Kyoto, Japan, May 2010, paper THPD046, pp. 4384–4386.
- [11] L. Faillace *et al.*, “Experimental results of carbon nanotube cathodes inside RF environment,” in *Proc. IPAC’15*, Richmond, VA, USA, May 2015, paper WEAD2, p. 2475.
- [12] R. B. Yoder, Z. Kabilova, and B. Saeks, “Electron beam generation and injection from a pyroelectric crystal array,” in *Proc. IPAC’16*, Busan, Korea, May 2016, paper TUPMY026, p. 1604.
- [13] T. Z. Fullem and Y. Danon, “Electrostatics of pyroelectric accelerators,” *J. Appl. Phys.*, vol. 106, p. 074101, 2009.
- [14] J. Hoffrogge *et al.*, “Tip-based source of femtosecond electron pulses at 30keV,” *J. Appl. Phys.*, vol. 115, p. 094506, 2014.
- [15] O. A. Louchev, S. Wada, N. Saito, H. Hatano, and K. Kitamura, “Pulsed laser operated high rate charging of Fe-doped LiNbO₃ crystal for electron emission,” *J. Appl. Phys.*, vol. 112, p. 073107, 2012.